

# Molecular BioSystems

Accepted Manuscript



This is an *Accepted Manuscript*, which has been through the Royal Society of Chemistry peer review process and has been accepted for publication.

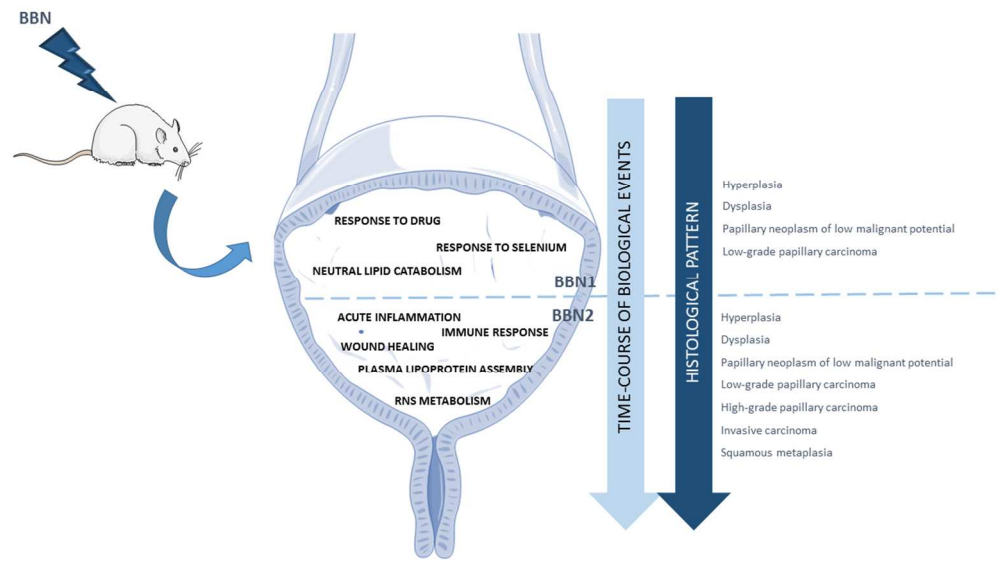
*Accepted Manuscripts* are published online shortly after acceptance, before technical editing, formatting and proof reading. Using this free service, authors can make their results available to the community, in citable form, before we publish the edited article. We will replace this *Accepted Manuscript* with the edited and formatted *Advance Article* as soon as it is available.

You can find more information about *Accepted Manuscripts* in the [Information for Authors](#).

Please note that technical editing may introduce minor changes to the text and/or graphics, which may alter content. The journal's standard [Terms & Conditions](#) and the [Ethical guidelines](#) still apply. In no event shall the Royal Society of Chemistry be held responsible for any errors or omissions in this *Accepted Manuscript* or any consequences arising from the use of any information it contains.



[www.rsc.org/molecularbiosystems](http://www.rsc.org/molecularbiosystems)



338x190mm (96 x 96 DPI)

**Comparative proteomic analyses of urine from rat urothelial carcinoma  
chemically induced by exposure to N-butyl-N-(4-hydroxybutyl)-nitrosamine**

Rita Ferreira<sup>1</sup>, Paula Oliveira<sup>2</sup>, Telma Martins<sup>1</sup>, Sandra Magalhães<sup>1</sup>, Fábio Trindade<sup>1</sup>,  
Maria João Pires<sup>2</sup>, Bruno Colaço<sup>2</sup>, António Barros<sup>1</sup>, Lúcio Santos<sup>3</sup>, Francisco Amado<sup>4</sup>,  
Rui Vitorino<sup>1,5</sup>

<sup>1</sup>QOPNA, Department of Chemistry, University of Aveiro, Portugal

<sup>2</sup>CITAB, Department of Veterinary Science, University of Trás-os-Montes e Alto  
Douro, Portugal

<sup>3</sup>Experimental Pathology and Therapeutics Group, Portuguese Institute of Oncology,  
Porto, Portugal

<sup>4</sup>QOPNA, School of Health Sciences, University of Aveiro, Portugal

<sup>5</sup>iBiMED, University of Aveiro, Portugal

**Corresponding author (✉):**

Rita Ferreira  
Chemistry Department, University of Aveiro  
Campus de Santiago  
3810-193 Aveiro  
Portugal  
e-mail: ritaferreira@ua.pt

Rui Vitorino  
Chemistry Department, University of Aveiro  
Campus de Santiago  
3810-193 Aveiro  
Portugal  
e-mail: rvitorino@ua.pt

**Running title:** Urinary proteomics in bladder cancer

**Key-words:** bladder cancer, GeLC-MS/MS, inflammation, multimarker strategies

**Abstract**

Bladder cancer is estimated to be the ninth most common malignancy with high rate of recurrence and progression despite therapy, being crucial its early diagnosis for timely interventions. Using a well-established animal model of urothelial carcinoma, we performed a comprehensive analysis of urine proteome profile from healthy animals and with urothelial carcinoma at two time-points of disease pathogenesis. GeLC-MS/MS followed by bioinformatic analysis of unique proteins and the ones present in significantly distinct levels among groups highlighted the biological processes involved in disease pathogenesis as, for instance response to selenium and to drug, neutral lipid metabolism at earlier stages of disease, and inflammation, immune response and wound healing at advanced stages. Proteins from the biological processes up-regulated in the urine of animals with urothelial carcinoma might be seen as putative disease biomarkers as, for example, cadherins, lipoproteins, and glycosyltransferases, to be included in multimarker strategies.

Taken together, data supports the application of urine proteomics for the identification of the biological processes modulated by bladder cancer in an integrative perspective. The present exploratory urinary proteomic analysis might be seen as an important starting point for studies targeting urinary proteins in human, aiming the implementation of novel laboratory approaches for the detection and successful management of urothelial carcinoma.

## Introduction

Urothelial bladder cancer is the 4<sup>th</sup> most common cancer in men and the 9<sup>th</sup> most common in women western world<sup>1, 2</sup>. Around 75% of newly diagnosed urothelial bladder cancer are noninvasive and have a high rate of recurrence and progression despite therapy<sup>1</sup>. So, there is a need for continuous surveillance of bladder cancer patients following initial treatment<sup>3</sup>. While histopathology of excised tumors or biopsy material and direct cystoscopy remain the gold standard for diagnosis and follow-up monitoring of bladder cancer, noninvasive diagnostic procedures are desirable<sup>2-4</sup>.

Screening of disease biomarkers in biofluids is a usual task in healthcare and disease prevention but is often hindered by sample complexity. Comparing to plasma, urine is less complex, containing approximately 3000 proteins, most of which are derived from the kidney and urinary tract<sup>5-7</sup>. Besides its lower complexity, the use of urine has many other advantages as a diagnostic tool, such as ease of sample acquisition, noninvasiveness avoiding patient discomfort and potential complications from an invasive procedure, and unrestricted quantities obtainable<sup>7-11</sup>. Once urine is in direct contact with bladder epithelia cells, it is a useful sample to study bladder diseases<sup>12</sup>. Some commercial tests have been developed to detect tumor-associated proteins released in urine such as tests for the monitoring of bladder tumor antigen (BTA) or of nuclear matrix protein 22 (NMP22/NUMA1); however, none of these tests can replace cystoscopy reviewed by<sup>4</sup>. So, the search for accurate and noninvasive tests continues with urinary proteomics gaining attention in bladder cancer research with the ultimate goal of biomarker discovery for screening/diagnosis<sup>2, 4, 12, 13</sup>.

The goal of our study was to characterize urinary protein profile modulated by urothelial carcinoma using GeLC-MS/MS, a strategy that combines one-dimensional SDS-PAGE with reversed phase-HPLC. To fulfill this goal, we utilized an animal model of urothelial carcinogenesis chemically induced by exposure to *N*-butyl-*N*-(4-hydroxybutyl)-nitrosamine (BBN), which reflects one of the most commonly occurring malignant tumors of the urinary tract<sup>14, 15</sup>. Proteome profiling of urine collected from healthy animals and with urothelial carcinoma (with distinct histological grades) followed by bioinformatic analysis allowed not only the identification of urinary proteins modulated by urothelial carcinoma, but also highlighted the biological

processes involved in disease pathogenesis, including lipid metabolism and response to selenium, inflammation, immune response and wound healing.

## Methods

### Animal protocol

The following protocol was approved by the Portuguese Ethics Committee for Animal Experimentation (*Direção Geral de Alimentação e Veterinária*, Approval no. 008962). Forty-five female Wistar rats were obtained at age of 5 weeks from Harlan (Barcelona, Spain). Rats were used in this study after a week of acclimation period. They were randomly housed 5-8 in a plastic cage, with hard wood chips for bedding, and maintained on a basal diet (Harlan Teklad, Global Diet). The room temperature and the relative humidity were controlled at  $22\pm 3^{\circ}\text{C}$  and  $60\pm 10\%$ , respectively. Fluorescent lighting was provided in a 12h light/dark cycle. BBN was purchased from Tokyo Kasei Kogyo (Japan) and administered in drinking water, in light impermeable bottles, at a concentration of 0.05%. Animals were divided in three groups and in two of them they were exposed to BBN during twenty consecutive weeks. Animals were observed daily for health check. Body weights, as well as food consumption, were measured weekly. The drinking solution was changed twice *per* week and the volume drunk was recorded. To evaluate histological changes induced in the urothelium by BBN treatment rats were killed twenty weeks after the beginning of carcinogen exposure (BBN1 group) or after twenty weeks of carcinogen exposure followed by eight weeks of tap water consumption (BBN2 group). At these time-points distinct histological grades of malignancy are expected<sup>16</sup>. Healthy animals were sacrificed at the same time points (CONT group). Rats were sacrificed with 0.4% sodium pentobarbital (1mL/Kg, intraperitoneal). Complete necropsies were carefully conducted. All organs were examined macroscopically for any changes. The urinary bladders were inflated *in situ* by injection of 10% phosphate buffered formalin (1mL), ligated around the neck to maintain proper distension and then were immersed in the same solution for 12 hours. After fixation, the formalin was removed; the urinary bladder was weighed and cut into four strips, and routinely processed for haematoxylin and eosin staining.

### Histopathological analysis

All sections were reviewed and the urothelial lesions staged by the World Health Organization/International Society of Urological Pathology consensus classification of urothelial (transitional cell) neoplasms of the urinary bladder. Urothelial lesions were categorized into either: as simple hyperplasia, nodular hyperplasia, dysplasia, carcinoma

in situ (CIS), papillary tumours, papillary neoplasm of low malignant potential, low-grade papillary carcinoma, high-grade papillary carcinoma, invasive carcinoma and epidermoid metaplasia.

### **Urine collection**

For urine collection, in the day before sacrifice, rats were individually placed on metabolic cages for 12 hours. Urine was centrifuged at 1000g for 10 min (4°C) and the supernatant was concentrated using a 10-kDa filter (Vivaspin 500-10kDa, Sartorius Biotech). The final retentate was resuspended in 100µL of 0.05M Tris and 2% SDS. Total protein content was estimated in the fraction corresponding to the retentate using the RC DC protein assay kit (Bio-Rad).

### **SDS-PAGE and *in-gel* digestion**

The proteome sample (50µg) was separated using SDS-PAGE in a 12.5% gel prepared as previously described<sup>17</sup>. The gel was stained with Colloidal Coomassie Blue G250. The samples were prepared in duplicate. Following SDS-PAGE of the protein samples, complete lanes were cut out of the gel and sliced into 16 sections. Each section was *in-gel* digested with trypsin. The resulting peptide mixture was then extracted from the gel fractions and dried using vacuum centrifugation.

### **LC-MS/MS analysis and protein ID**

The dried extracted peptides were dissolved in 10µL of mobile phase A (0.1% trifluoroacetic acid, 5% acetonitrile, 95% water). All peptide mixtures were analyzed in two separate times. The tryptic digests were then separated using an Ultimate 3000 (Dionex, Sunnyvale, CA) onto a 150mm × 75µm Pepmap100 capillary analytical C18 column with 3µm particle size (Dionex, LC Packings) at a flow rate of 300nL/min. The gradient started at 10min and ramped to 50% Buffer B (85% acetonitrile, 0.04% trifluoroacetic acid) over a period of 45min. The chromatographic separation was monitored at 214nm using a UV detector (Dionex/LC Packings) equipped with a 3nL flow cell. The peptides eluting from the column were mixed with a continuous flow of matrix solution (270nL/min, 2mg/mL α-CHCA in 70% ACN/0.3% TFA and internal

standard Glu-Fib at 15fmol) in a fraction microcollector (Probot, Dionex/LC Packings) and directly deposited onto the LC-MALDI plates at 20s intervals for each spot. Samples were analyzed using a 4800 MALDI-TOF/TOF Analyzer (AbSCIEX). A S/N threshold of 50 was used to select peaks for MS/MS analyses. The spectra were processed using the TS2Mascot (v1.0, Matrix Science Ltd) and submitted to Mascot software (v.2.1.0.4, Matrix Science Ltd) for peptide/protein identification. Searches were performed against the SwissProt protein database (March 2013) for *Rattus norvegicus*. Search was performed including data from all slices for global protein identification and emPAI calculation. A MS tolerance of 30ppm was found for precursor ions and 0.3Da for fragment ions, as well as two missed cleavages and methionine oxidation as variable modification. The confidence levels accepted for positive protein identification were  $p < 0.05$ . A false positive rate below 5% was obtained using a reverse database. Furthermore, proteins identified with one peptide were manually validated when MS/MS spectra presented at least 4 successive amino acids covered by *b* or *y* fragmentations.

### **Protein quantification and abundance measurement**

The abundance of identified proteins (common to all groups) was estimated by calculating the exponentially modified protein abundance index (emPAI)<sup>18</sup>. The emPAI is an exponential form of PAI<sup>-1</sup> (the number of detected peptides divided by the number of observable peptides *per* protein, normalized by the theoretical number of peptides expected via *in silico* digestion) defined as  $emPAI = 10^{PAI} - 1$  and the corresponding protein content in mole percent is calculated as  $mol \% = (emPAI / \sum emPAI) \times 100$ . Microsoft Office Excel was used to calculate the mole percent. The theoretically observable peptides were determined by the *in silico* digestion of mature proteins using from the output of the program Protein Digestion Simulator (<http://panomics.pnnl.gov/software/>). The observed peptides were unique parent ions including those with two missed cleavage. Mean protein emPAI values were log<sub>2</sub> transformed for protein ratio calculation.

### **Gelatine zymography**

Zymography assays were performed according to Caseiro et al.<sup>19</sup>. Briefly, the zymography was performed using a 10% SDS-PAGE separation gel with 0.1% of gelatine. Twenty micrograms of urinary protein from each group were incubated on charging buffer (100mM Tris pH 6.8, 5% SDS, 20% glycerol, 0.1% bromophenol blue) for 10 minutes, in a proportion of 1:1 (v/v). After the run, gels were incubated in renaturation buffer (2.5% Triton X-100) for 30 minutes, with soft agitation. Then, the zymo gels were changed to a development buffer (50mM Tris, 5mM NaCl, 10mM CaCl<sub>2</sub>, 1µM ZnCl<sub>2</sub>, 0.02% (v/v) Triton X-100, pH 7.4) for more 30 minutes, also with soft agitation. Finally, the gels were changed to a new development buffer, and incubated overnight at 37°C. For specific inhibition of metalloproteinases, zymograms were incubated in a solution containing 10mM EDTA. The zymo gels were stained with 0.12% (w/v) Coomassie Blue G250 prepared in 20% methanol, after 1 hour fixation in a solution of 10% acetic acid and 40% methanol. Gels were then destained with 25% methanol and scanned with Gel Doc XR System (Bio-Rad).

### **Immunoblotting analysis**

Immunoblotting analysis was performed according to Caseiro et al.<sup>20</sup>. In brief, concentrated urine samples were diluted in Tris buffered saline (TBS) to a final protein concentration of 0.01µg/µL and a volume of 100µL was slot-blotted into a nitrocellulose membrane (Hybond-ECL; Amersham Pharmacia Biotech, Buckinghamshire, UK). The membranes were blocked with 5% (w/v) dry non-fat milk in TBS-Tween (TBS-T) and then incubated overnight at 4°C with primary antibody (anti-osteopontin antibody (ab91655), anti-CRP antibody (C reactive protein; ab32412), or anti-IL-6 antibody (ab6672) from Abcam) diluted 1:1000 in blocking solution. The membranes were washed three times, ten minutes each, with TBS-T and incubated two hours with secondary antibody (horseradish-conjugated anti-rabbit, GE Healthcare, Buckinghamshire, UK) in a dilution of 1:1000. Detection was carried out with enhanced chemiluminescence according to manufacturer's instructions (GE Healthcare). Film images were acquired using GelDoc XR+ system (Bio-Rad, Hercules, CA.) and quantitative analysis of optical density (OD) was performed with QuantityOne<sup>®</sup> 1-D Analysis Software (Bio-Rad, Hercules, CA).

### Statistical Data analysis

Analysis of the statistical significance of differences between groups in relation to OD measures were performed with the GraphPad Prism version 5.0 for Windows (GraphPad Software, San Diego California, USA). Mean and standard deviation were calculated and a Kruskal-Wallis test followed by Dunn's multiple comparison post-hoc test was performed. Differences were considered statistically significant at p-values lower than 0.05. In case of protein data analysis, a CSV (comma separated values) dataset containing relevant information pertaining to all identified proteins was analyzed to extract meaningful information. An in-house developed C# program using LINQ (Language Integrated Query) (Microsoft Visual Studio 2012)<sup>©</sup> was used for data-mining the dataset. The output of the program has given several statistics which were then used by R Language scripts<sup>21</sup> to produce heatmaps and emPAI distribution facilitating the dataset analysis. The recovered statistics were: 1) dendrograms for normalized emPAI values in order to analyze their similarity/dissimilarity between groups (Figure 4), and 2) protein abundance ratio distribution as a function of each group (Figure 5).

## Results

During the experimental protocol all animals showed normal activity. Two animals from group BBN1 died during the experimental protocol, and therefore they were excluded from the study. Several biological variables were collected during the experimental protocol (Supplemental Table S1), which analysis evidenced a significantly lower body weight of BBN2 rats compared to age-matched CONT ones. Greyish-white urinary bladder masses varying in size from less than 1mm to masses that filled the entire lumen were observed, those in group BBN2 being the largest. The lesions were pedunculated with irregular surfaces and areas of necrosis, haemorrhage, and focal ulcerations. The lesions were distributed randomly throughout the entire urinary bladder. Stone formation in the urinary bladder was not observed in any rat. The incidence of histopathological lesions in each group is shown in Table 1. As can be depicted in this table, the prevalence of low-grade and high-grade papillary carcinoma, and invasive carcinoma was higher in the urinary bladder of BBN2 rats. No histopathological changes in urothelial cells were observed in CONT animals.

In order to identify urothelial carcinoma-related proteins in urine, we performed a large scale GeLC-MS/MS approach for quantitative comparison among animals. Two time points were considered for sample collection from healthy subjects (20 and 28 weeks) but for the purpose of the present study three groups of animals were considered according to the stage of tumoral lesions: 10 controls (CONT), animals with pre-malignant lesions (BBN1) and with malignant lesions (BBN2). CONT group included animals sacrificed after 20-weeks and 28-weeks of the beginning of the protocol. Desalted urine samples from all animals were analyzed by SDS-PAGE, and the results showed inter-individual biological variations (Supplemental Figure S1). For large-scale GeLC-MS/MS analysis five animals *per* group were selected for individual proteome characterization. Whole gel bands' analysis by LC-MS/MS retrieved 351 unique proteins (Supplemental Table S2). The majority of these proteins belong to metabolic processes, cellular processes as cell adhesion, cell communication and cell cycle. Regarding molecular function, an enrichment of proteins with catalytic activity and binding activity was noticed. Most of the identified proteins have intracellular origin (typically from cytoskeleton) (Figure 1).

Figure 2 illustrates the distribution of identified proteins *per* group. From all urinary proteins detected only 102 were common to all animals studied, including albumin, serine protease inhibitor, pro-epidermal growth factors, complement C3, alpha-1-macroglobulin, cadherin 1, IL-4 receptor, uromodulin, C-reactive protein and gelsolin. These common proteins are mainly involved in metabolic processes, immune system and response to stimulus. Sixty-one proteins were only identified in the urine of healthy animals, most of which related to metabolism. Twenty-three proteins were common to all animals with urothelial carcinoma, being the majority related to immune system (namely S100A9, glutathione-S-transferase and serum paraoxonase). In the urine of animals with the worst histological grade 83 unique proteins were identified whereas in the ones with less malignant lesions 55 were detected. Regarding the biological processes modulated by the disease, metabolism and cellular processes were the most prevalent (Supplemental Table S2).

In overall, the analysis of proteins *per* group evidenced an enrichment of unique proteins in the urine of animals with urothelial carcinoma at advanced states (83 in BBN2 *vs.* 55 in BBN1 *vs.* 61 in CONT). This variation might reflect the increased proteolytic activity noticed in BBN2 group (Supplemental Figure S3). Indeed, the analysis of urine gelatinolytic proteases' profile revealed two zymo gel bands with more activity in the urine of animals from BBN2 group, one with approximately 66 kDa (band 1, Figure 3) and other of approximately 30 kDa (band 3, Figure 3). A band with approximately 45 kDa (band 2) was only noticed in the urine of BBN2 rats. Considering the molecular weight (MW), one might suspect of MMP-2 (predicted MW of 66 kDa) or pro-MMP-2 (predicted MW of 72 kDa), and of kallikrein-1 (predicted MW of 29 kDa), previously reported in urine<sup>19</sup>. Once the appearance of the 45 kDa band was concomitant to MMP-2 activation, we might suspect that band 2 results from the truncation of membrane type 1 (MT1)-MMP, as previously suggested for bladder cancer<sup>22</sup>.

The inter-individual analysis of identified proteins in each group evidenced a lower variation of the urinary proteome among animals from BBN2 group, in opposite to the observed in BBN1 animals (Supplemental Figure S1). Protein-protein interaction analysis of unique proteins within groups evidenced in BBN2 an enrichment of proteins involved in the regulation of blood coagulation, regulation of IL-1 production, regulation of immunoglobulin production and secretion, ATP biosynthetic processes,

cellular monovalent cation homeostasis, negative regulation of proteolysis, negative regulation of appetite and response to nutrient levels. In BBN1 group there was a prevalence of proteins related to neutral lipids catabolism, negative regulation of Ras, response to selenium and calcium dependent adhesion. Contrarily, in healthy animals there was a prevalence of proteins associated with renal and glomerular filtration, nerve growth factor signaling and response to platelet-derived growth factor stimulus (Supplemental Figure S4).

The hierarchical comparative analysis of the common proteins based on emPAI values was pictured in a heatmap based on their normalized abundances (Figure 4) and two main clusters (BBN2 and BBN1 vs. BBN1 and CONT) were highlighted. Moreover, two main distinct protein nodes might be observed. Node 1 comprises three smaller nodes which include proteins involved in metabolism and immune system (node 1.1), cellular processes (node 1.2) and immune system and response to stimulus (node 1.3). Node 2 includes two smaller nodes, metabolic processes (node 2.1) and transport and immune system (node 2.2). As can be depicted in Figure 4, node 2.2 is up-regulated in animals with urothelial carcinoma. This cluster includes albumin, IgG2A, alpha-1B-glycoprotein, fetuin and transferrin. Node 2.1 is down-regulated in controls and in some BBN1 animals. Alpha-1-macroglobulin, hemopexin, fibronectin, T-kininogen 1, ceruloplasmin and murinoglobulin-1 are the proteins included in this cluster. An enrichment of other proteins was noticed. For instance, major urinary protein is in higher levels in the urine of healthy animals.

Normalized abundance analysis evidenced hemoglobin, albumin and Ig lambda-2 chain C region as the most abundant proteins in BBN1 and BBN2 groups, and Ig kappa chain C region, major urinary protein and Cu/Zn superoxide dismutase as the lowest abundant ones (Figure 5). In order to validate emPAI data of urine proteome, immunoblotting analysis of target proteins was performed and data obtained highlight a similar trend to emPAI distribution (Supplemental Figure S5). Protein-protein interaction analysis performed with ClueGo+CluePedia<sup>23</sup> of the proteins present in significantly distinct amounts in the urine of rats with urothelial carcinoma highlighted the prevalence of cellular response to IL-1, acute-phase response, acute inflammatory response, phospholipid and lipoprotein organization and metabolism (normalized values higher than 1.3). Negative regulation of carbohydrate metabolic proteins is among the

biological processes down-represented (normalized values lower than -1.3) in the urine of rats with lower histological grade of malignancy (Supplemental Figure S6).

In order to obtain an integrated perspective of all the pathways modulated by urothelial carcinoma at different stages of disease, protein-protein interaction analysis was performed with ClueGo+CluePedia considering the unique proteins identified in each group and the ones found in significant distinct levels (Figure 6). In BBN1 (green nodes), there was an up-regulation of neutral lipid catabolic process, response to selenium ions and response to drug. In BBN2 (blue nodes), it was noticed a prevalence of acute inflammation and immune response, wound healing and plasma lipoprotein assembly. Preliminary findings from our research group on the analysis of urine proteome from bladder cancer patients confirms the involvement of these biological processes in disease pathogenesis (Supplemental Figure S8).

## Discussion

Our study highlights the impact of urothelial carcinoma progression on urinary proteome allowing the improved elucidation of disease pathogenesis, and the envisioning of potential disease biomarkers with screening/diagnosis value. A large scale GeLC-MS/MS strategy was used to analyze the urinary proteome of rats with chemically induced urothelial carcinoma, a well-established animal model of bladder cancer<sup>16</sup>. Indeed, BBN-induced tumors in rats are equivalent to the non-muscle-invasive urothelial carcinoma clinically observed in humans<sup>14, 24, 25</sup>. Animal models of urothelial carcinoma offer several advantages in medical research<sup>16</sup> as the possibility to follow-up tumors development and relate it with urine proteome dynamics. Histological examination of bladder confirmed the greater incidence of low- and high-grade papillary carcinoma, and invasive carcinoma in BBN2 compared to BBN1 animals. These histological changes were further related with the negative regulation of appetite and response to nutrient levels (Supplemental Figure S3), supporting the bladder cancer-related cachexia previously reported<sup>26</sup>.

Urine proteome analysis highlighted an integrated perspective of the molecular pathways underlying the progression of urothelial carcinoma (Figure 6). In the urine of animals with lower histological grade of malignancy it was noticed an up-regulation of the biological processes cellular response to drug and response to selenium ions (green nodes, Figure 6). Selenoproteins are known to participate in the response to oxidative stress, in the regulation of redox balance and of various metabolic and developmental processes<sup>27</sup>. Proteins involved in glutathione metabolism as glutathione S-transferase (GST) and LanC-like protein 1 that binds glutathione were detected in the urine of BBN1 animals. Several isoforms of GST were identified, including GST alpha 1, GST alpha 4 and GST P (Supplemental Table S2), with higher levels of GST Mu1 detected in the urine of BBN1 rats. Regulation of GST has been studied in the context of bladder cancer once this superfamily of enzymes protects normal cells by catalyzing conjugation reactions of electrophilic compounds, including carcinogens, to glutathione. Some GST enzymes possess antioxidant activity against hydroperoxides<sup>28</sup>. Thioredoxin is a defensive protein induced by various stresses and has anti-oxidative, anti-apoptotic and anti-inflammatory effects<sup>29</sup>, being also involved in cell's response to the carcinogen.

The up-regulation of lipid metabolism was also noticed in animals with lower histological grade of malignancy. Among the proteins identified, considerable attention has been given to lipoproteins due to its potential role in angiogenesis. Increased urinary levels of apolipoproteins as apoA1, apoA2, apoC3 and apoE were already reported in bladder cancer, being apoA1 and apoA2 suggested as novel candidate urine biomarkers for bladder cancer<sup>12</sup>. However, apoA1 was also reported to be up-regulated in diabetic rat bladders due to inflammation<sup>30</sup>, being no specific marker of bladder cancer. The presence of fatty acid-binding protein (FABP4) in the urine of BBN1 rats also supports bladder cancer-induced white adipose tissue (WAT) to brown adipose tissue (BAT) remodeling, which precludes cachexia<sup>31</sup>.

Inflammation, immune response and wound healing were among the biological processes found more prevalent in animals with the higher histological grade of malignancy (BBN2, blue nodes, Figure 6). Data supports bladder cancer has a highly immunogenic malignancy. Urothelial cancer cells seem to manipulate the immune system by inhibiting its cytotoxic function while stimulating the secretion of growth promoting factors<sup>32</sup>. The importance of inflammatory cytokines as IL-1 $\beta$  and IL-6 in maintaining tumor cell growth and viability is well established. IL-6 and IL-1 $\beta$  produced by inflammatory cells, such as T cells and macrophages, endothelial cells, fibroblasts and some cancer cells, stimulate hepatocytes to synthesize C-reactive protein (CRP), which, in turn, activates the complement system. Moreover, IL-6 was already suggested to function as an autocrine growth factor for bladder carcinoma cells<sup>33</sup>. The presence of class I histocompatibility antigen, Non-RT1.A alpha-1 chain (RT1-Aw2), and carcinoembryonic antigen CGM1 (Ceacam3), which are involved in the regulation of T cell mediated cytotoxicity and in the regulation of T cell proliferation, respectively<sup>34</sup>, supports the tumor-promoting effects of T cells in bladder cancer, as previously suggested<sup>35</sup>. The up-regulation of wound healing reflects an attempt of the organism to resolve inflammation. Proteolytic enzymes are involved in this biological process through the modulation of extracellular matrix<sup>36</sup>. Overexpression of MMPs in tumors and in stroma can lead to increased MMPs activities in various body fluids as in urine. MMPs, as MMP-2, were previously detected in the urine of patients suffering bladder cancer<sup>37</sup>. Cathepsin D, another protease identified in the urine of BBN2 rats, might degrade the protein components of the matrix and free growth factors therein embedded, thus favoring tumor growth, invasion and angiogenesis<sup>38</sup>. Nevertheless,

increased proteolysis in urine is not an exclusive feature of cancer being also related to other diseases as diabetes mellitus<sup>19</sup>.

Inflammation is related to the disruption of the glycocalyx in vascular tissue<sup>36</sup>, which might justify the presence of several glycosylated proteins (according to Uniprot) in the urine of animals with the higher histological grade of malignancy. Aberrant glycosylation has been related to the development and progression of cancer. Some glycosyltransferases were detected in the urine of BBN2 animals, including dolichyl-diphosphooligosaccharide-protein glycosyltransferase subunit 2 (RPN2), an essential subunit of the N-oligosaccharyl transferase (OST) complex and UDP-glucose:glycoprotein glycosyltransferase 1 (UGT1). P-glycoprotein is a known target of RPN2-induced glycosylation, regulating tumor cells' sensitivity to drugs<sup>39</sup>. UGT1 can selectively reglycosylate an *N*-linked glycan according to the conformation of the protein bearing. This glycosyltransferase has a striking substrate specificity, preferring near-native molten globule-like folding intermediates and orphan subunits, instead of native or extensively misfolded proteins. For instance, UGT1 is involved in MHC class I molecules maturation and assembly<sup>40</sup>. According to STRING analysis (data not shown), RPN2 and UGT1 might share substrates as calnexin precursor, integral membrane protein 1 and mannosyl oligosacchareide glucosidase.

In conclusion, GeLC-MS/MS profiling of urine applied to the study of urothelial carcinoma highlighted the mechanisms involved in disease pathogenesis as, for instance inflammation, immune response and wound healing. Such analysis presents the added dimension of giving an integrated perspective of the molecular events underlying the progression of urothelial carcinoma, with urinary proteins from several biological processes presenting potential diagnosis value. Data here presented might be an important starting point for studies targeting specific urinary proteins in human, aiming the development of multimarker strategies for the screening/diagnosis of urothelial carcinoma.

### **Clinical Perspectives**

The profiling of urine proteome allows the characterization of the biological processes involved in the pathogenesis of urothelial carcinoma. The simultaneous analysis of

protein targets from the processes modulated by the disease will certainly improve specificity and sensibility in the diagnosis and monitoring of bladder cancer.

#### **Author contribution**

Rita Ferreira – data analysis and writing; Paula Oliveira - animal model, tumor histology; Telma Martins – proteome analysis; Sandra Magalhães – proteome analysis; Fábio Trindade – proteome analysis; Maria João Pires – animal model; Bruno Colaço – animal model; António Barros – bioinformatics, data analysis; Lúcio Santos – translation to clinics; Francisco Amado – data analysis; Rui Vitorino – proteome and data analysis, writing

## Acknowledgments

This work was supported by Portuguese Foundation for Science and Technology (FCT), European Union, QREN, FEDER and COMPETE for funding the QOPNA research unit (project PEst-C/QUI/UI0062/2013; FCOMP-01-0124-FEDER-037296) and the research project (PTDC/DES/114122/2009; FCOMP-01-0124-FEDER-014707), and by RNEM (Portuguese Mass Spectrometry Network).

## References

1. M. Burger, J. W. Catto, G. Dalbagni, H. B. Grossman, H. Herr, P. Karakiewicz, W. Kassouf, L. A. Kiemeny, C. La Vecchia, S. Shariat and Y. Lotan, *European urology*, 2013, 63, 234-241.
2. T. Lei, X. Zhao, S. Jin, Q. Meng, H. Zhou and M. Zhang, *Clinical genitourinary cancer*, 2013, 11, 56-62.
3. C. J. Bischoff and P. E. Clark, *Current opinion in oncology*, 2009, 21, 272-277.
4. V. Urquidi, C. J. Rosser and S. Goodison, *Current medicinal chemistry*, 2012, 19, 3653-3663.
5. V. Thongboonkerd and P. Malasit, *Proteomics*, 2005, 5, 1033-1042.
6. C. L. Chen, T. S. Lin, C. H. Tsai, C. C. Wu, T. Chung, K. Y. Chien, M. Wu, Y. S. Chang, J. S. Yu and Y. T. Chen, *J Proteomics*, 2013, 85, 28-43.
7. H. Husi, J. B. Barr, R. J. Skipworth, N. A. Stephens, C. A. Greig, H. Wackerhage, R. Barron, K. C. Fearon and J. A. Ross, *International journal of proteomics*, 2013, 2013, 760208.
8. F. E. Ahmed, *J Chromatogr B Analyt Technol Biomed Life Sci*, 2009, 877, 1963-1981.
9. V. Thongboonkerd, *Molecular bioSystems*, 2008, 4, 810-815.
10. J. Wu, Y. D. Chen and W. Gu, *J Zhejiang Univ Sci B*, 11, 227-237.
11. P. Lescuyer, D. Hochstrasser and T. Rabilloud, *J Proteome Res*, 2007, 6, 3371-3376.
12. Y. T. Chen, C. L. Chen, H. W. Chen, T. Chung, C. C. Wu, C. D. Chen, C. W. Hsu, M. C. Chen, K. H. Tsui, P. L. Chang, Y. S. Chang and J. S. Yu, *Journal of proteome research*, 2010, 9, 5803-5815.
13. R. T. Bryan, W. Wei, N. J. Shimwell, S. I. Collins, S. A. Hussain, L. J. Billingham, P. G. Murray, N. Deshmukh, N. D. James, D. M. Wallace, P. J. Johnson, M. P. Zeegers, K. K. Cheng, A. Martin and D. G. Ward, *Proteomics. Clinical applications*, 2011, 5, 493-503.
14. P. A. Oliveira, F. Adegas, C. A. Palmeira, R. M. Chaves, A. A. Colaco, H. Guedes-Pinto, P. L. De la Cruz and C. A. Lopes, *International journal of experimental pathology*, 2007, 88, 39-46.
15. M. Roupert, R. Zigeuner, J. Palou, A. Boehle, E. Kaasinen, R. Sylvester, M. Babjuk and W. Oosterlinck, *European urology*, 2011, 59, 584-594.
16. P. A. Oliveira, A. Colaco, P. L. De la Cruz and C. Lopes, *Experimental oncology*, 2006, 28, 2-11.
17. U. K. Laemmli, *Nature*, 1970, 227, 680-685.
18. Y. Ishihama, Y. Oda, T. Tabata, T. Sato, T. Nagasu, J. Rappsilber and M. Mann, *Mol Cell Proteomics*, 2005, 4, 1265-1272.
19. A. Caseiro, R. Ferreira, C. Quintaneiro, A. Pereira, R. Marinheiro, R. Vitorino and F. Amado, *Clinical biochemistry*, 2012, 45, 1613-1619.

20. A. Caseiro, A. Barros, R. Ferreira, A. Padrao, M. Aroso, C. Quintaneiro, A. Pereira, R. Marinheiro, R. Vitorino and F. Amado, *Translational research : the journal of laboratory and clinical medicine*, 2013, DOI: 10.1016/j.trsl.2013.09.005.
21. R. D. C. Team, 2011.
22. K. Saeb-Parsy, A. Veerakumarasivam, M. J. Wallard, N. Thorne, Y. Kawano, G. Murphy, D. E. Neal, I. G. Mills and J. D. Kelly, *British journal of cancer*, 2008, 99, 663-669.
23. G. Bindea, J. Galon and B. Mlecnik, *Bioinformatics*, 2013, DOI: 10.1093/bioinformatics/btt019.
24. C. Palmeira, P. A. Oliveira, R. Arantes-Rodrigues, A. Colaco, P. L. De la Cruz, C. Lopes and L. Santos, *Oncology reports*, 2009, 21, 247-252.
25. C. Palmeira, P. A. Oliveira, C. Lameiras, T. Amaro, V. M. Silva, C. Lopes and L. Santos, *Oncol Lett*, 2010, 1, 373-377.
26. A. I. Padrao, P. Oliveira, R. Vitorino, B. Colaco, M. J. Pires, M. Marquez, E. Castellanos, M. J. Neuparth, C. Teixeira, C. Costa, D. Moreira-Goncalves, S. Cabral, J. A. Duarte, L. L. Santos, F. Amado and R. Ferreira, *The international journal of biochemistry & cell biology*, 2013, 45, 1399-1409.
27. E. Reszka, *Clinica chimica acta; international journal of clinical chemistry*, 2012, 413, 847-854.
28. T. Simic, A. Savic-Radojevic, M. Pljesa-Ercegovac, M. Matic and J. Mimic-Oka, *Nature reviews. Urology*, 2009, 6, 281-289.
29. O. N. Spindel, C. World and B. C. Berk, *Antioxidants & redox signaling*, 2012, 16, 587-596.
30. E. Yohannes, J. Chang, G. J. Christ, K. P. Davies and M. R. Chance, *Molecular & cellular proteomics : MCP*, 2008, 7, 1270-1285.
31. J. M. Argiles, C. C. Fontes-Oliveira, M. Toledo, F. J. Lopez-Soriano and S. Busquets, *Journal of cachexia, sarcopenia and muscle*, 2014, DOI: 10.1007/s13539-014-0154-x.
32. G. Gakis, *Advances in experimental medicine and biology*, 2014, 816, 183-196.
33. K. Saito and K. Kihara, *International journal of urology : official journal of the Japanese Urological Association*, 2013, 20, 161-171.
34. K. Kuespert, S. Pils and C. R. Hauck, *Curr Opin Cell Biol*, 2006, 18, 565-571.
35. Z. Zhu, Z. Shen and C. Xu, *Mediators of inflammation*, 2012, 2012, 528690.
36. B. L. Brucher and I. S. Jamall, *BMC cancer*, 2014, 14, 331.
37. M. A. Mohammed, M. F. Seleim, M. S. Abdalla, H. M. Sharada and A. H. Abdel Wahab, *BMC urology*, 2013, 13, 25.
38. G. Nicotra, R. Castino, C. Follo, C. Peracchio, G. Valente and C. Isidoro, *Cancer biomarkers : section A of Disease markers*, 2010, 7, 47-64.
39. K. Honma, K. Iwao-Koizumi, F. Takeshita, Y. Yamamoto, T. Yoshida, K. Nishio, S. Nagahara, K. Kato and T. Ochiya, *Nature medicine*, 2008, 14, 939-948.
40. W. Zhang, P. A. Wearsch, Y. Zhu, R. M. Leonhardt and P. Cresswell, *Proceedings of the National Academy of Sciences of the United States of America*, 2011, 108, 4956-4961.

**Table 1:** Incidence of urothelial lesions.

	CONT	BBN1	BBN2
<b>Histological lesion</b>	<b>H<sub>2</sub>O</b>	<b>20 weeks of BBN</b>	<b>20 weeks of BBN + 8 weeks of H<sub>2</sub>O</b>
Normal urothelium	20/20 (100%)	0 (0%)	0(0%)
Simple hyperplasia	0 (0%)	8/10 (80%)	11/13(85%)
Nodular hyperplasia	0 (0%)	9/10 (90%)	13/13(100)
Papilar hyperplasia	0(0%)	9/10(90%)	9/13(70%)
Dysplasia	0 (0%)	9/10(90%)	10/13(76.9%)
CIS	0 (0%)	0(0%)	0(0%)
Papilloma	0 (0%)	6/10(60%)	3/13(23%)
Papillary neoplasm of low malignant potential	0 (0%)	5/10(50%)	8/13(61.5%)
Low-grade papillary carcinoma	0 (0%)	5/10(50%)	11/13(84.6%)
High-grade papillary carcinoma	0 (0%)	1/10(10%)	10/13(76.9%)
Invasive carcinoma	0 (0%)	3/10(30%)	5/13(38.5%)
Epidermoid metaplasia	0 (0%)	1/10(10%)	9/13(70%)

## Figure legends

**Figure 1:** Protein annotation in GO terms using PANTHER according to Biological Process (A), Molecular Function (B) and Cellular Location (C).

**Figure 2:** Venn diagram highlighting the distribution of identified proteins *per* group (CONT, BBN1 and BBN2) evidencing the overlapped and unique proteins. (<http://bioinfogp.cnb.csic.es/tools/venny/index.html>).

**Figure 3:** Representative zymography for urine samples of CONT, BBN1 and BBN2 groups (A). Optical density measurements of proteolytic bands 1 and 3 (B).

(\* $p < 0.05$  vs. CONT; \*\* $p < 0.01$  vs. CONT; \*\*\*  $p < 0.001$  vs. CONT).

**Figure 4:** Heatmap representing the clustering of subject groups showing five main nodes related to the biological processes: metabolism and immune system, cellular processes, response to stimuli and immune system, metabolism and immune system, and transport and immune system. Color from green to red represents low to high protein abundance.

**Figure 5:** Normalized abundance of urinary proteins in BBN1 (A) and BBN2 (B) groups. Protein accession number has correspondence to protein name at Supplemental Table S2.

**Figure 6:** ClueGo+CluePedia analysis of protein-protein interaction considering unique proteins and common proteins present in significant distinct levels (based on emPAI values) in the urine of CONT, BBN1 and BBN2 animals. Blue nodes refer to the biological processes up-regulated in BBN2, green nodes refer to the ones up-regulated in BBN1 and red nodes refer to the ones up-regulated in CONT. Nodes size and colour intensity reflect the number of associated proteins. (Supplemental Figure S7 summarizes the processes up-regulated in BBN1 (A) and in BBN2 (B)).

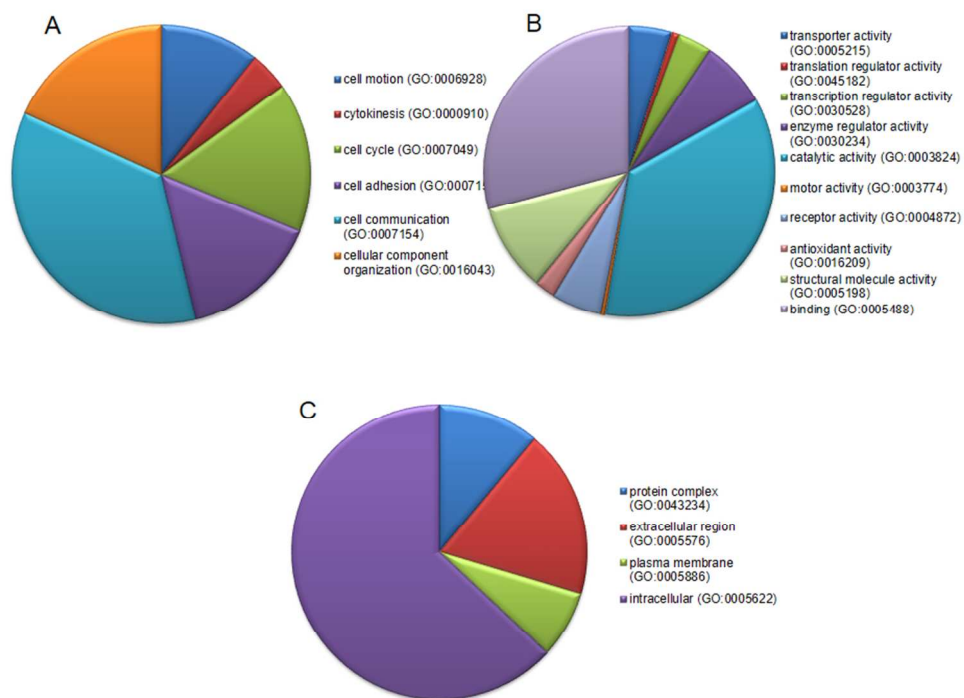


Figure 1: Protein annotation in GO terms using PANTHER according to Biological Process (A), Molecular Function (B) and Cellular Location (C).  
254x190mm (96 x 96 DPI)

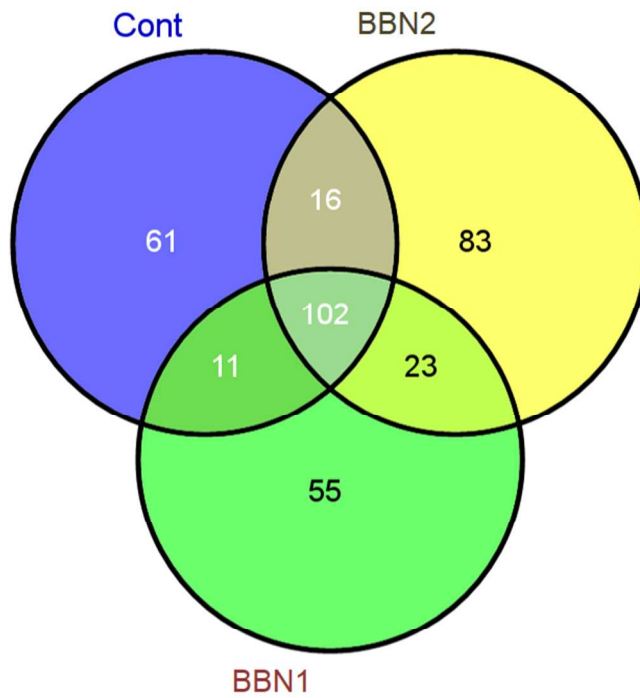


Figure 2: Venn diagram highlighting the distribution of identified proteins per group (CONT, BBN1 and BBN2) evidencing the overlapped and unique proteins. (<http://bioinfogp.cnb.csic.es/tools/venny/index.html>).  
254x190mm (96 x 96 DPI)

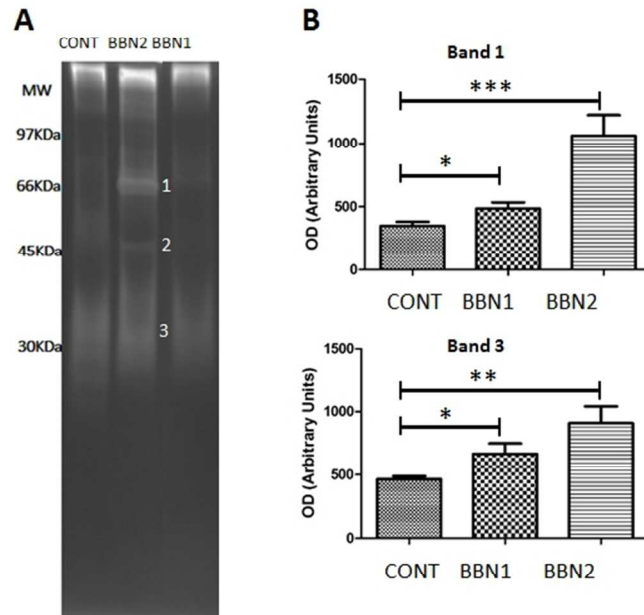


Figure 3: Representative zymography for urine samples of CONT, BBN1 and BBN2 groups (A). Optical density measurements of proteolytic bands 1 and 3 (B). (\*p < 0.05 vs. CONT; \*\*p<0.01 vs. CONT; \*\*\* p < 0.001 vs. CONT).

211x158mm (96 x 96 DPI)

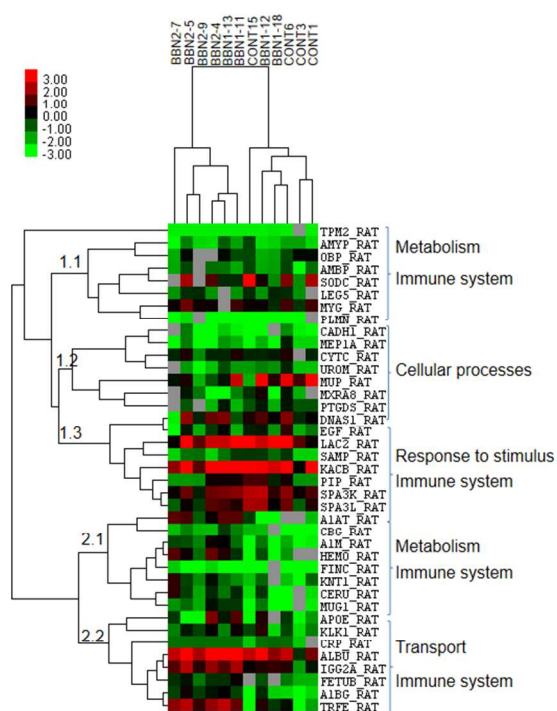


Figure 4: Heatmap representing the clustering of subject groups showing five main nodes related to the biological processes: metabolism and immune system, cellular processes, response to stimuli and immune system, metabolism and immune system, and transport and immune system. Color from green to red represents low to high protein abundance.

254x190mm (96 x 96 DPI)

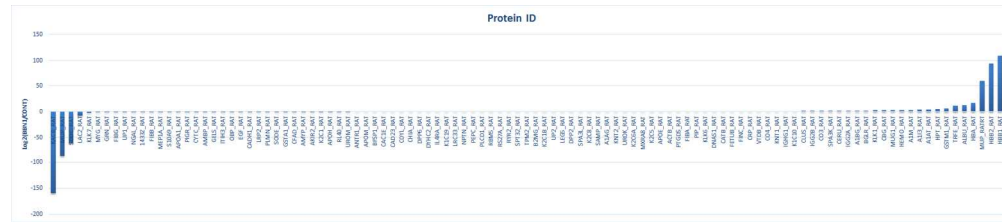




Figure 5: Normalized abundance of urinary proteins in BBN1 (A) and BBN2 (B) groups. Protein accession number has correspondence to protein name at Supplemental Table S2.

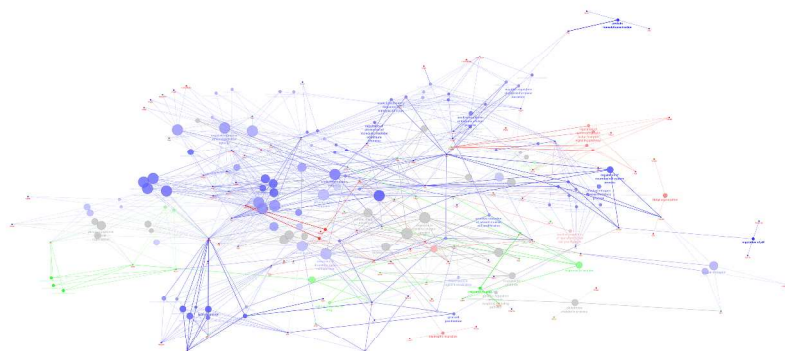


Figure 6: ClueGo+CluePedia analysis of protein-protein interaction considering unique proteins and common proteins present in significant distinct levels (based on emPAI values) in the urine of CONT, BBN1 and BBN2 animals. Blue nodes refer to the biological processes up-regulated in BBN2, green nodes refer to the ones up-regulated in BBN1 and red nodes refer to the ones up-regulated in CONT. Nodes size and colour intensity reflect the number of associated proteins. (Supplemental Figure S7 summarizes the processes up-regulated in BBN1 (A) and in BBN2 (B)).  
1668x783mm (72 x 72 DPI)